

# The Free Transmission Problem for a Water Droplet

Dirk Langemann

Rostock university, department of mathematics, D-18051 Rostock, Germany  
`dirk.langemann@mathematik.uni-rostock.de`

**Abstract.** Water droplets on insulating material influence strongly the aging process of the material and the material loses its hydrophobic and insulating properties. The shape of the droplets signifies the state of the aging material. The present paper discusses a numerical procedure to calculate the droplet shape in an electric field generated by constant voltage between two electrodes. This leads to a transmission problem on the free surface of the droplet. It contains two sub-problems, first finding the droplet shape in a given electric field via an evolution problem, and second calculating the electric field for a given droplet shape via finite elements. The force density acting on the droplet shape depends on the electric field, and the electric field depends on the droplet shape. Both sub-problems have to be solved simultaneously. The typical shapes of the droplets are shown for several voltages. Finally a comparison between the behaviours of a dielectric droplet of pure rainwater and a conductive droplet of water with environmental additives is presented.

## 1 Introduction

Water droplets on insulating material influence strongly the aging process of the material and the material loses its hydrophobic and insulating properties. This process causes considerable problems in the maintenance of high voltage power lines. The shape of the droplets signifies the state of the aging material, [6]. A first step to understand the effects of the aging process to the droplet shapes, is the determination of the droplet behaviour within electric fields.

The present paper considers a single droplet in an electric field as it has been used in the experiments in [6]. The water droplet lays on a solid support made of resin, and the electric field is generated by a voltage between two electrodes inside the resin. If a voltage is applied, the droplet becomes lengthened and flattened. In particular, it loses axis-symmetry. But the electric field is depending on the droplet shape too and on the conductive properties of the water. This feed-back leads to a free boundary value problem, comp. [13].

In [10] and [12] the problem was numerically handled by finite integration techniques, comp. [11], on a three-dimensional equidistant grid in a harmonic quasi-stationary formulation. Here we concentrate in particular on the variable shapes of the droplets. Thus, finite elements on a triangulation adapted to the droplet shape are used for the calculation of the electric potential.

The realistic situation of a three-dimensional droplet in an alternating electric field involves various effects like material flux inside the droplet fluid, inertial effects, induced currents in the fluid and so on. All these effects are regarded to be rather small, see [10]. Hence, only stationary electric fields are considered here.

Further, the restriction to a two-dimensional droplet does not avoid any specific difficulty. The handling of the free boundary value problem by a Banach-like iteration proposed in [2] can be transferred to the three-dimensional droplet as well with some technical effort but without fundamental changes of the numerical procedure. Here, we focus on the numerics of the free boundary value problem of a droplet in a stationary electric field consisting in an iteration alternating between two sub-problems: Those are an evolution problem for calculating the droplet shape, see Sec. 3 and a finite element computation for determining the electric field, see Sec. 4.

The main ideas of the iteration are presented in Sec. 2 together with a detailed model set-up. In Sec. 3, the equilibrium of forces on the upper boundary of the droplet and in the triple points is discussed. The droplet shape is computed via an evolution problem modeling a hypothetical transient motion of the droplet. Sec. 4 presents the details in the computation of the electric potential and of the force density on the droplet boundary caused by the electric field.

In Sec. 5, we compare the dielectric and the conductive droplet. On the one hand, pure rainwater is nearly not conductive. On the other hand, environmental additives pollute the water. It gets conductive. The droplet shapes are given for both situations and various voltages. We will shortly present the further ideas to handle a droplet of rainwater with a very small limited amount of additives, i. e. the case that the fluid is an imperfect conductor.

## 2 Problem Set-up

### 2.1 Model Description and Notations

We investigate a two-dimensional water droplet in a stationary electric field. The droplet is described by its upper boundary  $\Gamma$  which is given in polar co-ordinates with the origin  $O$ , i. e.  $\Gamma = \{x_\Gamma = (r(\varphi) \cos \varphi, r(\varphi) \sin \varphi); \varphi \in [0, \pi]\}$ . The angle  $\varphi$  serves as parameter of the points  $x_\Gamma(\varphi)$  at the boundary. The droplet fluid is in fact rainwater with the mass density  $\delta = 1000 \text{ kgm}^{-3}$  and the surface tension  $\alpha = 0.072 \text{ Nm}^{-1}$ . The surface tension does not depend on the electric field here. The voltage generating the electric field is  $2U$ . The boundary of the electrodes is called  $\Gamma_1$ , see Fig. 1. The points  $A$  and  $B$  are used in Sec. 3.1. The positions of the electrodes inside the resin influence obviously the occurring numerical values.

The dielectricity of rainwater is  $\varepsilon_{\text{H}_2\text{O}} = 81$  and the dielectricity of the solid support made of resin is  $\varepsilon_2 = 4$ . The dielectricity of the the air is  $\varepsilon_1 = 1.0006 \approx 1$ , what is an acceptable approximation for our purposes.

The electric field causes a concentration  $\rho$  of electric charge at the boundary  $\Gamma$  of the droplet. In the case of a dielectric droplet, this charge is effected by

polarization, and in the case of a conductive droplet, there is free electric charge at the boundary. This distinction is discussed in Sec. 4.1. The concentration of electric charge at  $\Gamma$  results in a force density  $p_e(\varphi) = p_e(x_\Gamma(\varphi))$  there.

## 2.2 Fundamental Iteration

The free boundary value problem consists in two sub-problems. The first sub-problem of finding the droplet shape described by  $r(\varphi)$  for a given force density  $p_e(\varphi)$  is called  $\mathcal{R}$ -problem. The second sub-problem of finding  $p_e$  for a given  $r$  is referred to as  $\mathcal{P}$ -problem. There are two operators  $\mathcal{R}$  and  $\mathcal{P}$  mapping a force density  $p_e$  to a resulting  $r$  and vice versa, a given  $r$  to a force density  $p_e$ , i. e.

$$\mathcal{R} : p_e \rightarrow r \text{ and } \mathcal{P} : r \rightarrow p_e .$$

While solving the problem of a stationary droplet in the electric field, we are searching for a fixed point of the combined operator  $\mathcal{R}\mathcal{P}$ , i. e.  $r_{\text{fix}} = \mathcal{R}\mathcal{P}r_{\text{fix}}$ .

To separate both sub-problems we state the Banach-like iteration

$$r^{(i+1)} = \omega \mathcal{R}\mathcal{P}r^{(i)} + (1 - \omega)r^{(i)} \quad (1)$$

with the relaxation parameter  $\omega$ . The iteration (1) is a standard procedure in the solution of free boundary value problems, cf. [13]. It was successfully applied for the closed osmometer problem in [2]. The basic ideas of the convergence proof from [2] can be transferred to the present problem. So, we assume

$$\lim_{i \rightarrow \infty} r^{(i)} = r_{\text{fix}} \text{ (point-wise)} \quad (2)$$

at least for suitable  $\omega$  and the tests presented in Sec. 5 show that (2) holds.

## 3 The $\mathcal{R}$ -Problem of Calculating the Droplet Shape

### 3.1 The Equilibrium of Forces at the Droplet Boundary

The forces acting in  $x_\Gamma(\varphi)$  with  $\varphi \in (0, \pi)$  at the upper boundary of the droplet in the direction of the outer normal  $n$  on  $\Gamma$  are the capillary pressure  $p_k$ , the pressure  $p_h$  depending on the depth of water, a pressure  $p_0$  serving as penalty parameter to hold the droplet volume constant and the outer force density  $p_e$  causes by the electric field. The droplet is stationary, if the equilibrium of forces

$$0 = p_k(\varphi) + p_h(\varphi) + p_0(\varphi) + p_e(\varphi) \quad (3)$$

holds in every point  $x_\Gamma(\varphi)$  with  $\varphi \in (0, \pi)$  except in the corners  $P = x_\Gamma(0)$  and  $P' = x_\Gamma(\pi)$ . The capillary pressure is given by

$$p_k(\varphi) = -\alpha \cdot \kappa(\varphi) \text{ with } \kappa(\varphi) = \frac{r(\varphi)^2 + 2r'(\varphi)^2 - r(\varphi)r''(\varphi)}{(r(\varphi)^2 + r'(\varphi)^2)^{\frac{3}{2}}}$$

depending on the curvature  $\kappa$  of the droplet shape, comp. [4]. The pressure inside the droplet depending on the depth of the water is

$$p_h(\varphi) = \delta g(h - r(\varphi) \sin \varphi) \quad \text{with} \quad h = \max_{\varphi \in [0, \pi]} r(\varphi) \sin \varphi.$$

The penalty pressure  $p_0$  acts against a volume dilatation and is expressed by

$$p_0 = \left( \frac{V}{V_r} - 1 \right) p_{\text{air}} \quad \text{with} \quad V_r = \frac{1}{2} \int_0^\pi r(\varphi)^2 d\varphi \quad (4)$$

with an assumed volume  $V$  of the undeformed droplet fluid under the air pressure  $p_{\text{air}}$ . Equation (4) replaces the constraint condition of incompressibility in the present formalism of equilibrated forces.

In the corner  $P$  the surface tension  $\alpha$  acts between the fluid and the air in the direction  $PB$ . The boundary tension  $\alpha_{1,2}$  is the difference in first the surface tension between the solid support and the fluid in the direction  $PA$  and second the small boundary tension between the solid and the air. This leads to a constant angle between the droplet shape and the support, comp. [4]. We use the angle  $\vartheta = 1.1$  and state in the corners  $P$  and  $P'$  the equations

$$\tan \vartheta \cdot r'(0) + r(0) = 0 \quad \text{and} \quad \tan \vartheta \cdot r'(\pi) - r(\pi) = 0. \quad (5)$$

In [8] investigations of the behaviour of the electric potential near the corner points, [9], show that additional forces to disturb the equilibrium of forces in the corners, do not occur within the present problem.

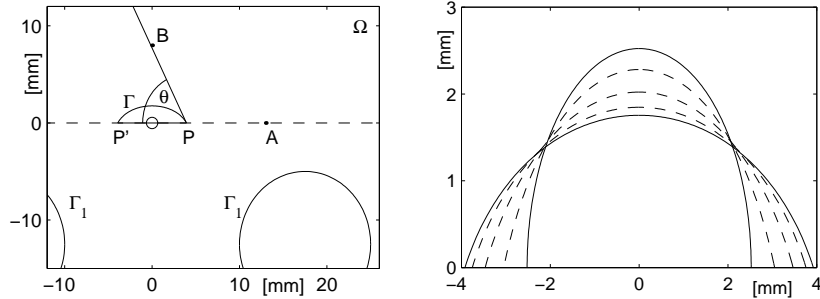


**Fig. 1.** Left : Model set-up of the problem. The droplet lays in the centre on the surface of the solid support containing two electrodes. Right : Evolution of the radius in the evolution problem starting with  $r(\varphi) = \text{const.}$  and setting  $p_e \equiv 0$ . The solid lines mark the initial and final shape of the droplet. The dashed lines give the radius at the auxiliary time-instants  $t = 2 \cdot 10^{-5} \text{ s}$ ,  $t = 6 \cdot 10^{-5} \text{ s}$  and  $t = 10 \cdot 10^{-5} \text{ s}$  (from above). The height is four times exaggerated, cf. Fig. 2 for a droplet with low distortion in scale.

### 3.2 Numerics of the Evolution Problem

Equation (3) with the boundary conditions (5) is an ordinary non-linear elliptic boundary value problem for  $r(\varphi)$  on  $\varphi \in [0, \pi]$ , comp. [3]. It can be solved by computing the respective parabolic problem with an auxiliary time  $t$ . That is

$$\frac{\partial}{\partial t} r(\varphi, t) = p_k(\varphi) + p_h(\varphi) + p_0(\varphi) + p_e(\varphi), \quad (6)$$

$$\frac{\partial}{\partial t} r(0, t) = k[\tan \vartheta \cdot r'(0, t) + r(0, t)] \quad \text{and} \quad \frac{\partial}{\partial t} r(\pi, t) = -k[\tan \vartheta \cdot r'(\pi, t) - r(\pi, t)] \quad (7)$$

where  $r'(\cdot, t)$  denotes the derivative with respect to the first, local parameter  $\varphi$ , and  $k$  is a suitable amplification factor, e. g.  $k = \pi \frac{\alpha}{2V}$ . The factor  $k$  equilibrates the evolution speed of the droplet boundary inside the interval  $\varphi \in (0, \pi)$  and on its ends and makes the solution of (6) numerically more convenient.

Equations (6-7) can be discretized over  $\varphi$ , s. [1], and solved by standard methods for stiff ordinary differential equations, [5], like e. g. `ode15s` in `Matlab`. In the examples of Sec. 5 the interval  $[0, \pi]$  was discretized into 200 equidistant grid points. Here a time-constant radius is reached in less than  $1 \cdot 10^{-3}$  s, cf. Fig. 1.

## 4 The $\mathcal{P}$ -Problem of Calculating the Electric Potential

### 4.1 The Electric Potential and the Electric Force Density

In the first case of a dielectric droplet, the support  $\Omega^{(1)}$  of the electric field  $E^{(1)}$  is whole the plane outside the electrodes. In the second case of a conductive droplet, the droplet is free of an electric field, and  $\Omega^{(2)}$  is the plane outside the electrodes and outside the droplet. Furthermore the domains are each free of electric charge and the potentials are vanishing at the boundaries  $\partial\Omega^{(1)}$  and  $\partial\Omega^{(2)}$ . The fact that the potential  $\Phi^{(2)}$  vanishes on the boundary of a conductive droplet follows from the symmetry of the problem. It holds  $E^{(i)}(x) = -\nabla\Phi^{(i)}(x)$ . We get two boundary value problems, cf. [7], for  $i = 1, 2$

$$\begin{aligned} -\nabla \cdot [\varepsilon(x)\nabla\Phi^{(i)}(x)] &= 0 && \text{in } x \in \Omega^{(i)}, \\ \Phi^{(i)}(x) &= 0 && \text{on } x \in \partial\Omega^{(i)} \setminus \Gamma_1, \\ \Phi^{(i)}(x) &= \text{sign}(x_1) \cdot U && \text{on } x \in \Gamma_1. \end{aligned} \quad (8)$$

The position depending dielectricity  $\varepsilon(x)$  with  $x = (x_1, x_2)^T$  is  $\varepsilon_1$  in the air,  $\varepsilon_2$  in the support and  $\varepsilon_{H_2O}$  inside the droplet, s. Sec. 2. Problem (8) is linear in  $U$ .

In the case of a conductive droplet, we assume temporarily free electric charge  $\rho(x) = \varepsilon_0 \nabla \cdot E^{(2)}(x)$  in a limit layer on the droplet boundary, and the force density acting on the droplet boundary is found by integration in normal direction

$$p_e^{(2)}(\varphi) = \lim_{\nu \rightarrow 0} \int_{-\nu}^{\nu} \rho(x_\Gamma + \sigma n) E^{(2)}(x_\Gamma + \sigma n) d\sigma = \frac{1}{2} \varepsilon_0 \left( \frac{\partial \Phi^{(2)}(x_\Gamma)}{\partial n} \right)^2 \quad (9)$$

corresponding to [4] and [12].

In the case of a dielectric droplet, the normal component of the electric field  $E^{(1)}$  jumps at the boundary of the droplet and causes a concentration of polarized charge  $\rho_P(x) = \varepsilon_0 \nabla \cdot E^{(1)}(x)$ . The force density acting on the droplet boundary is found similarly to (9) by

$$p_e^{(1)}(\varphi) = \frac{1}{2} \varepsilon_0 \left[ \left( \frac{\partial \Phi^{(1)}(x_\Gamma)}{\partial n^+} \right)^2 - \left( \frac{\partial \Phi^{(1)}(x_\Gamma)}{\partial n^-} \right)^2 \right] \quad (10)$$

with the normal derivatives  $\partial/\partial n^+$  outside the droplet and  $\partial/\partial n^-$  inside the droplet. Hence, the force density  $p_e$  can be calculated in both cases depending on the droplet shape which determines the domain  $\Omega^{(2)}$  resp. the dielectricity  $\varepsilon(x)$  in  $\Omega^{(1)}$ . Since the potential  $\Phi^{(2)}$  is vanishing inside the conductive droplet, (9) and (10) express identical facts although the physical background is well different.

## 4.2 Finite Elements and Numerical Treatment

Using the symmetry, we consider (8) only in the right half-plane. The half-plane is restricted by a rectangle. The error due to the restriction is regarded to be small because of the local character of any disturbance of the electric field.

The boundary value problem (8) with its Dirichlet boundary conditions is solved by standard finite elements on a triangulation, which is refined near the boundary of the droplet, cf. Fig. 2. It is created once in a pre-processing and adapted to each actual shape of the droplet.

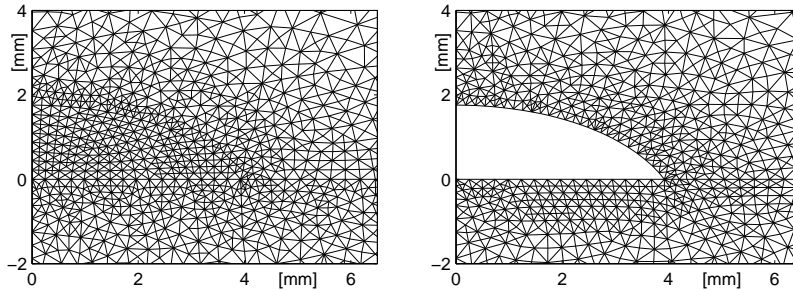


**Fig. 2.** Details of the triangulations, left : dielectric droplet, right : conductive droplet. Both contain a droplet under the absence of an electric field.

In the presented examples triangulations with 9011 points and about 17600 triangles were used. That leads to  $\approx 50$  triangles sharing a side with the discretized boundary of the droplet. The resulting system of linear equations is solved by standard procedures for sparse matrices. The solution was checked with the ones on different triangulations and regarded to be just fine.

## 5 Comparison of Dielectric and Conductive Droplets

The iteration (1) to find a fixed-point of the operator  $\mathcal{RP}$  works rather fast. For low voltages  $U < 10$  kV, it needs about five steps with  $\omega = 1$ . Higher voltages require a smaller relaxation parameter and needed up to 20 steps. One step on the triangulation given in Sec. 4.2 takes about 90 s on a 2 GHz machine. It contains the solution of the Dirichlet problem (8) on the pre-processed triangulation for the shape given by  $r^{(i)}$ , calculating  $p_e$ , solving the evolution problem (6) to find  $r^{(i+1)}$  and adapting the triangulation to the new droplet shape.

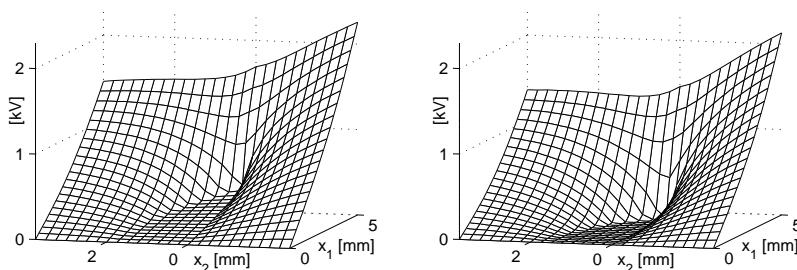


**Fig. 3.** Potentials (details) near the droplet for  $U = 8$  kV, left : dielectric, right : conductive droplet. Refraction is remarkable at the interface of the support and the air.

The potentials  $\Phi^{(1)}$  and  $\Phi^{(2)}$  are presented in Fig. 3. The difference between them is small, but  $\Phi^{(1)}$  is not zero inside the dielectric droplet. On the other hand, the droplet shapes differ very well for larger voltages. Fig. 4 shows typical droplet shapes for both cases.

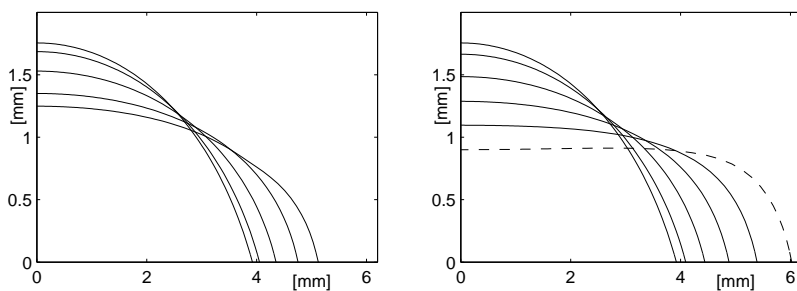


**Fig. 4.** Droplet shapes for  $U = 0$  kV,  $U = 8$  kV,  $U = 16$  kV,  $U = 24$  kV and  $U = 32$  kV (solid lines, from above), left : dielectric droplet, right : conductive droplet. The additional dashed line shows the droplet shape for  $U = 40$  kV. Vertical scale  $\approx 8:1$ , horizontal scale  $\approx 16:1$ , i. e. two times exaggerated height.

An example of a droplet shape in a very strong electric field, here for  $U = 40$  kV is given in Fig. 4. The droplet has become lengthened and flattened so clearly, that a local height minimum is remarkable in  $x_1 = 0$ . For even higher voltages the droplet will tear up. The numerical values of the voltages depend on the positions of the electrodes. For instance, electrodes at larger distances from the droplet require higher voltages to produce the same effects.

Fig. 5 gives a closer comparison between the dielectric and the conductive droplet. The conductive droplet becomes more lengthened and more flattened for the same voltage. The difference has an essential magnitude for strong electric fields.

The shapes of the droplets are identical for  $U$  and  $-U$ . This makes clear why the droplets oscillate with double the frequency of a slowly alternating voltage.

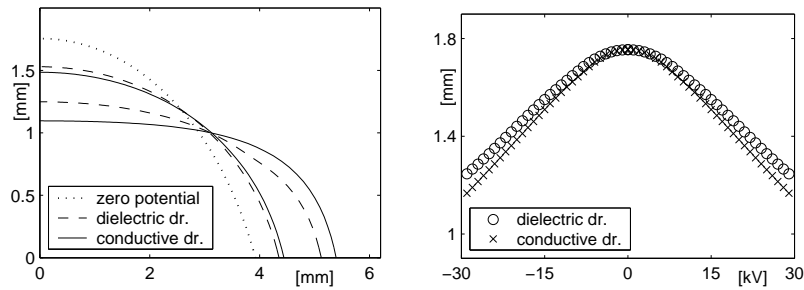


**Fig. 5.** Left : Droplet shapes for  $U = 16$  kV and  $U = 32$  kV (dashed lines : dielectric, solid lines : conductive droplet). Right : Droplet heights depending on the voltage  $U$ .

The assumptions of a purely dielectric and a purely conductive droplet are idealizations. A realistic droplet of rainwater contains a limited amount of free electric charge. For low voltages, it behaves like a purely conductive droplet. For higher voltages, all free electric charge will be concentrated on the boundary. Nevertheless, it does not suffice to assure the absence of an electric field inside the droplet for higher voltages. The droplet behaves more and more like a dielectric one.

To handle this situation numerically, a further evolution equation for the flux of the free electric charge on the boundary of the droplet has to be solved under the constraint condition of a limited amount of free electric charge. Instead of the stationary problem (8), a quasi-stationary problem including charge flux and a dependence of the conductivity on the available electric charge has to be solved.

## 6 Conclusion

The free boundary value problem of determining the shape of a rainwater droplet in a stationary electric field was handled by a Banach-like iteration over two sub-

problems. The first sub-problem is an evolution problem to find the droplet shape for a given outer force density. The second sub-problem consists in finding the electric potential and thus the force density. It was computed by finite elements.

We resume that the proposed numerical procedure works fine in the two-dimensional case without further sophistication. An extension to the three-dimensional case is actually in work and requires technical effort on the base of the same ideas. Thus, the numerical techniques to calculate the shapes of droplets on insulating material are presented and tested.

The difference between the shapes of dielectric and conductive droplets is remarkable. A discussion of experimental results should include this material property.

## References

1. Ames, W. F.: Numerical Methods for Partial Differential Equations. Academic Press, Boston (1992)
2. Frischmuth, K., Hänler, M.: Numerical Analysis of the Closed Osmometer Problem. ZAMM **79**(2) (1999) 107-116
3. Fucik, S., Kufner, A.: Nonlinear Differential Equations. Elsevier, Amsterdam (1980)
4. Grimsehl, E.: Lehrbuch der Physik **1**, (Course on theoretical physics, Vol. 1). Teubner, Leipzig (1987)
5. Hairer, E., Wanner, G.: Solving Ordinary Differential Equations **2**, Stiff and Differential-Algebraic Problems. Springer, Berlin (1991)
6. Keim, S., König, D.: Study of the Behavior of Droplets on Polymeric Surfaces under the Influence of an Applied Electrical Field. Proc. IEEE Conference on Electrical Insulation and Dielectric Phenomena, Austin, October 17-20 (1999) 707-710
7. Landau, L. D., Lifschitz, E. M.: The classical theory of fields. Butterworth, Washington DC (1997)
8. Langemann, D.: A Droplet in a Stationary Electric Field. Mathematics and Computers in Simulation (to appear 2003)
9. Mazja, V. G., Nazarov, S. A., Plamenevskij, B. A.: Asymptotic theory of elliptic boundary value problems in singularly pertubated domains. Birkhäuser, Basel (2000)
10. van Rienen, U., Clemens, M. Wendland, T.: Simulation of Low-Frequency Fields on Insulators with Light Contaminations. Proc. IEEE Transactions on Magnetics **32**(3) (1996) 816-819
11. van Rienen, U.: Lineare Gleichungssysteme in der numerischen Feldberechnung (Systems of linear equations in the numerical computation of fields). Habilitation, TU Darmstadt (1996)
12. Schreiber, U., van Rienen, U.: Simulation of the Behavior of Droplets on Polymeric Surfaces under the Influence of an Applied Electrical Field. Proc. 9<sup>th</sup> Biennial IEEE Conference, CEFC 2000, June 4-7 Milwaukee (2000)
13. Sethian, J. A.: Level set methods: evolving interfaces in geometry, fluid mechanics, computer vision and material science. Cambridge Univ. Press, Cambridge (1998)